Major-element geochemistry of pelites

Jacob B. Forshaw[1,2] and David R.M. Pattison[1]
[1]Department of Geoscience, University of Calgary, Calgary, Alberta T2N 1N4, Canada
[2]Institut für Geologie, Universität Bern, Bern 3012, Switzerland

ABSTRACT

Pelites (shales and mudstones) are arguably the most important rock type for interpreting metamorphism. Their significance derives from their widespread occurrence and the range of mineral assemblages they develop at different conditions of pressure and temperature. We compiled a global database of 5729 major-element whole-rock analyses of pelites from different metamorphic grades (shales to granulite-facies paragneisses) to (1) determine an average composition, (2) examine the range and variability in their composition, and (3) assess if there is evidence for grade-related geochemical changes. Median values are given instead of average values to eliminate the effect of extremes. The median worldwide pelite is as follows (anhydrous, values in wt%): $SiO_2 = 64.13$, $TiO_2 = 0.91$, $Al_2O_3 = 19.63$, $FeO^{total} = 6.85$, $MnO = 0.08$, $MgO = 2.41$, $CaO = 0.65$, $Na_2O = 1.38$, and $K_2O = 3.95$. The median $X_{Mg} = MgO/(MgO + FeO^{total})$ in moles is 0.39. The median $X_{Fe3+} = 2 \times Fe_2O_3/(2 \times Fe_2O_3 + FeO)$ in moles was measured in 1964 samples and is 0.23. On an Al_2O_3-FeO-MgO (AFM) diagram, the median worldwide pelite plots within a strong clustering of analyses between X_{Mg}^{proj} = projected molar $MgO/(MgO + FeO^{total}) = 0.30–0.55$ (median = 0.42) and A^{Ms} = molar $[Al_2O_3 – (3 \times K_2O)]/[Al_2O_3 – (3 \times K_2O) + FeO^{total} + MgO] = 0.0–0.4$ (median = 0.19). Pelites show a continuous decrease in volatile content with increasing metamorphic grade and a decrease in X_{Fe3+} from the diagenetic to biotite zone. Lower median SiO_2 values and higher median Al_2O_3 and A^{Ms} values in the porphyroblast and subsolidus sillimanite or K-feldspar zones, as well as higher median MnO values in the garnet zone, may reflect sampling bias or metasomatism.

INTRODUCTION

Metapelites are metamorphosed clay-rich sedimentary rocks (e.g., shales and mudstones). They are widespread in the rock record, and ever since the pioneering work of George Barrow (1893), they have been useful as indicators of metamorphic grade because their mineral assemblages are sensitive to changing pressure and temperature (*P-T*) conditions (Hietanen, 1967; Pattison and Tracy, 1991; Spear, 1993). Several compilations of the geochemical compositions of metapelites have been assembled and their values compared to those of unmetamorphosed shales (Shaw, 1956; Ague, 1991). Numerous studies have calculated phase diagrams for an "average" pelite composition, as a means to infer representative *P-T* conditions of commonly occurring metapelitic mineral assemblages, and to compare *P-T* conditions in different metamorphic belts around the world (Mahar et al., 1997; Tinkham et al., 2001; Caddick and Thompson, 2008; White et al., 2014; Pattison and Spear, 2018; Forshaw and Pattison, 2021). However, these average pelite compositions are rarely the same, making strict comparisons difficult. Thus, there remains uncertainty over what truly is an average pelite, and how much compositional variability pelites show.

A related topic of debate is the degree to which elements are redistributed during the devolatilization that accompanies prograde metamorphism (Ague, 1991; Stepanov, 2021). While mass transfer of major elements can be significant in domains of high fluid flux (e.g., veins, skarns, and sometimes along lithologic contacts), mass transfer away from these domains is thought to be broadly negligible (Ague, 2011, 2017). Despite this, small variations in several of the most important major elements (e.g., Al, K, Mg, Fe²⁺, and Fe³⁺) can lead to different mineral compositions, proportions, and, in turn, assemblages (Spear, 1993). Therefore, it is important to assess the degree of major-element mobility during prograde metamorphism, since this underpins our assumption that a single bulk composition can be used for phase diagram calculations across a range of metamorphic grades.

We present a new compilation of published pelitic whole-rock analyses ranging in metamorphic grade from shales to granulite-facies gneisses. It is ~20 times larger than any previous compilation. We used this database to document the range in chemical compositions of pelites, provide an average pelite composition, and assess whether there are any significant compositional changes as a function of metamorphic grade.

NEW COMPILATION OF LITERATURE DATA

Several previous studies compiled bulk compositional data from the literature in order to assess major-element compositions of pelites and possible changes with metamorphic grade (Lapadu-Hargues, 1945; Shaw, 1956; Ague, 1991). Since these studies, the number of published pelitic whole-rock analyses in the literature has increased considerably, and many unpublished theses containing analyses are now available online. Using these, we constructed a new database of 5729 analyses from 364 studies categorized into 103 regions. Only individual rock samples that had been crushed and analyzed using bulk techniques such as wet chemistry or X-ray fluorescence (XRF) were included. Samples from domains of high fluid flux (e.g., described as selvedge or coming from vein margins) were excluded from the database because they have been subject to localized mass transfer. The following major rock-forming components were analyzed in all samples: SiO_2, TiO_2, Al_2O_3, FeO, MnO, MgO, CaO, Na_2O, and K_2O. Where reported by the authors of the previous studies, we also included determinations of P_2O_5, Fe_2O_3, and loss-on-ignition (LOI). For wet chemical analyses, we combined H_2O, CO_2, and SO_3 together as an estimate for LOI (e.g., volatile content), as was done by Ague (1991). The Supplemental
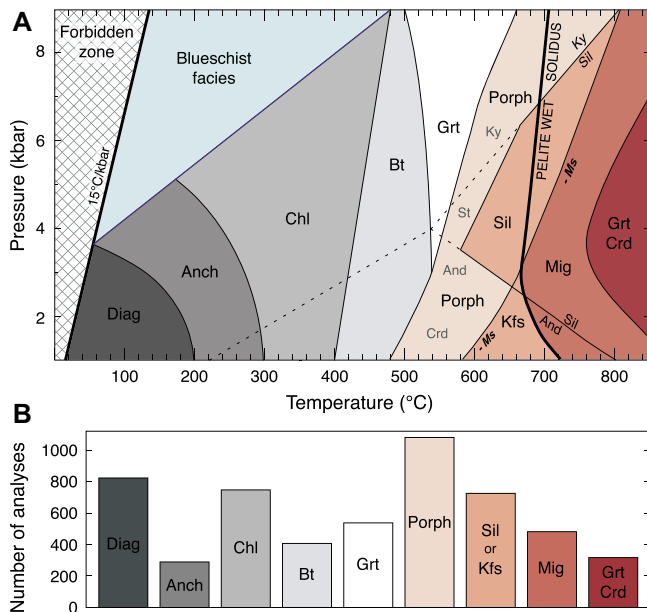
Figure 1. (A) Pressure-temperature distribution of metapelitic zones used in this study: diagenetic (Diag), anchizone (Anch), chlorite (Chl), biotite (Bt), garnet (Grt), porphyroblast (Porph), subsolidus sillimanite or K-feldspar (Sil-Kfs), migmatite (Mig), and garnet-cordierite (Grt-Crd). Other mineral abbreviations are after Warr (2021). (B) Histogram of the number of analyses in each zone.

Material[1] describes in detail the methodology used to exclude nonpelitic analyses; categorize the samples according to metamorphic grade; and portray the data in Al_2O_3-FeO-MgO (AFM) diagrams involving compositional projection. A complete catalog listing all analyses, including the sample name, metamorphic zone, literature reference, and whole-rock data in weight percent, is available in the Supplemental Material.

Due to the large number of analyses in the database, we were able to divide the samples into finer-scale metamorphic grade–related categories than previous studies (cf. Shaw, 1956; Ague, 1991) while maintaining >250 analyses in each category (Fig. 1). Nine zones were defined: diagenetic, anchizone, chlorite, biotite, garnet, porphyroblast, subsolidus sillimanite or K-feldspar, migmatite, and garnet-cordierite. The diagenetic zone refers to samples described as unmetamorphosed shales and mudstones, while the anchizone and chlorite zones refer to low-grade shales and/or slates classified using illite or chlorite crystallinity (Merriman and Frey, 1999). Higher-grade zones were based on the appearance of index minerals. The porphyroblast zone refers to muscovite-bearing, sillimanite-absent mineral assemblages containing combinations of cordierite, staurolite, andalusite, and kyanite, with or without garnet. Although the stability of these mineral assemblages varies with pressure, they typically develop in a relatively narrow range of metamorphic grade (approximately equal to metamorphic temperature), upgrade of the consumption of chlorite and downgrade of the development of sillimanite or K-feldspar (Fig. 1). The subsolidus sillimanite or K-feldspar zone includes muscovite + sillimanite–bearing mineral assemblages and, at low pressure, subsolidus K-feldspar–bearing mineral assemblages, which develop at different pressures but at similar metamorphic grade. The migmatite zone includes mineral assemblages in suprasolidus rocks that contain combinations of garnet, cordierite, sillimanite, and K-feldspar but lack coexisting garnet and cordierite. In total, 308 samples could not be classified into one of these zones.

TREATMENT OF DATA
Projections

Projection of bulk compositions into an AFM diagram (Fig. 2A; Thompson, 1957) permits visualization of the variation in the three main compositional variables of pelites, namely, Al, Fe, and Mg. It also allows the compositional effects of varying modal proportions of quartz and plagioclase feldspar in the original sedimentary protolith to be filtered out. Whole-rock analyses comprising 9–12 components (see above) were reduced to the six-component KFMASH (K_2O-FeO-MgO-Al_2O_3-SiO_2-H_2O) system using projections from apatite, ilmenite, albite, and anorthite to remove P_2O_5, TiO_2, Na_2O, and CaO, respectively. All iron was assumed to be FeO (ferrous), and MnO was omitted. To plot the KFMASH analyses in an AFM diagram, further projection from quartz (SiO_2), hydrous fluid (H_2O), and either muscovite or K-feldspar (K_2O) was required. Given that the majority of samples in the database were muscovite-bearing samples, the AFM diagram in Figure 2A shows all sam-

ples projected from muscovite (A^{Ms}). Figure S2 includes diagrams projected from K-feldspar, as well as diagrams separating lower-grade, muscovite-bearing samples from higher-grade, K-feldspar–bearing samples.

Statistical Analysis

Geoscientists commonly use the mean and standard deviation to describe the compositional variation in major-element geochemical data sets. However, of the various methods used to assess "average" values, the mean and standard deviation consistently perform the worst because they are the most susceptible to outliers (Rock, 1988; Woronow and Love, 1990). Therefore, we used the median and the interquartile range as the most representative measures of the average and the spread of the whole database, as well as subsets of data. When assessing possible grade-related variations, the mean is additionally shown for comparison (Fig. 3). Compositional data are inherently multivariate, have a constant sum, and in turn are constrained by the closure problem (Rollinson and Pease, 2021). To ensure that correlations observed in our grade-related assessment did not result from the interdependence of weight percent oxide values (Chayes, 1960), we transformed compositional data using $\log_{10}$ compositional mass ratios (Aitchison, 1982). Drawbacks of this approach are that a choice must be made for the conserved element in the ratios, and that log ratios are sometimes difficult to interpret. We found that trends between log ratio and weight percent oxide graphs were similar (Fig. S3), and thus we only show weight percent oxide values in Figure 3.

COMPOSITIONAL VARIABILITY
AFM Diagrams

Of the 5729 analyses, 409 plotted at anomalously low or high A^{Ms} values (>1.0 or <−0.4; A^{Ms} = molar $[Al_2O_3 − (3 × K_2O)]/[Al_2O_3 − (3 × K_2O) + FeO^{total} + MgO]$), and those are not shown in Figure 2A. Most analyses plotted between $X_{Mg}^{proj} = 0.30$–0.55 [X_{Mg}^{proj} = projected molar $MgO/(MgO + FeO^{total})$] and $A^{Ms} = 0.0$–0.4, with our median worldwide pelite plotting at $X_{Mg}^{proj} = 0.42$ and $A^{Ms} = 0.19$ (Fig. 2A; Table 1). There was a strong clustering midway between the AFM plotting positions of garnet and chlorite in the AFM diagram and no clear distinction between high- and low-Al pelites (cf. Spear, 1993, his figure 10-3; see Fig. 2A herein).

Ferric Iron

There were 1964 analyses in the database for which FeO was measured using titration, permitting an estimate of the whole-rock ferrous/ferric iron ratio. Figure 2B shows that most analyses plotted between $X_{Mg}^* = 0.30$–0.55 [$X_{Mg}^* =$ molar $MgO/(MgO + FeO)$] and $X_{Fe3+} = 0.1$–0.3 [$X_{Fe3+} = 2 × Fe_2O_3/(2 × Fe_2O_3 + FeO)$], with
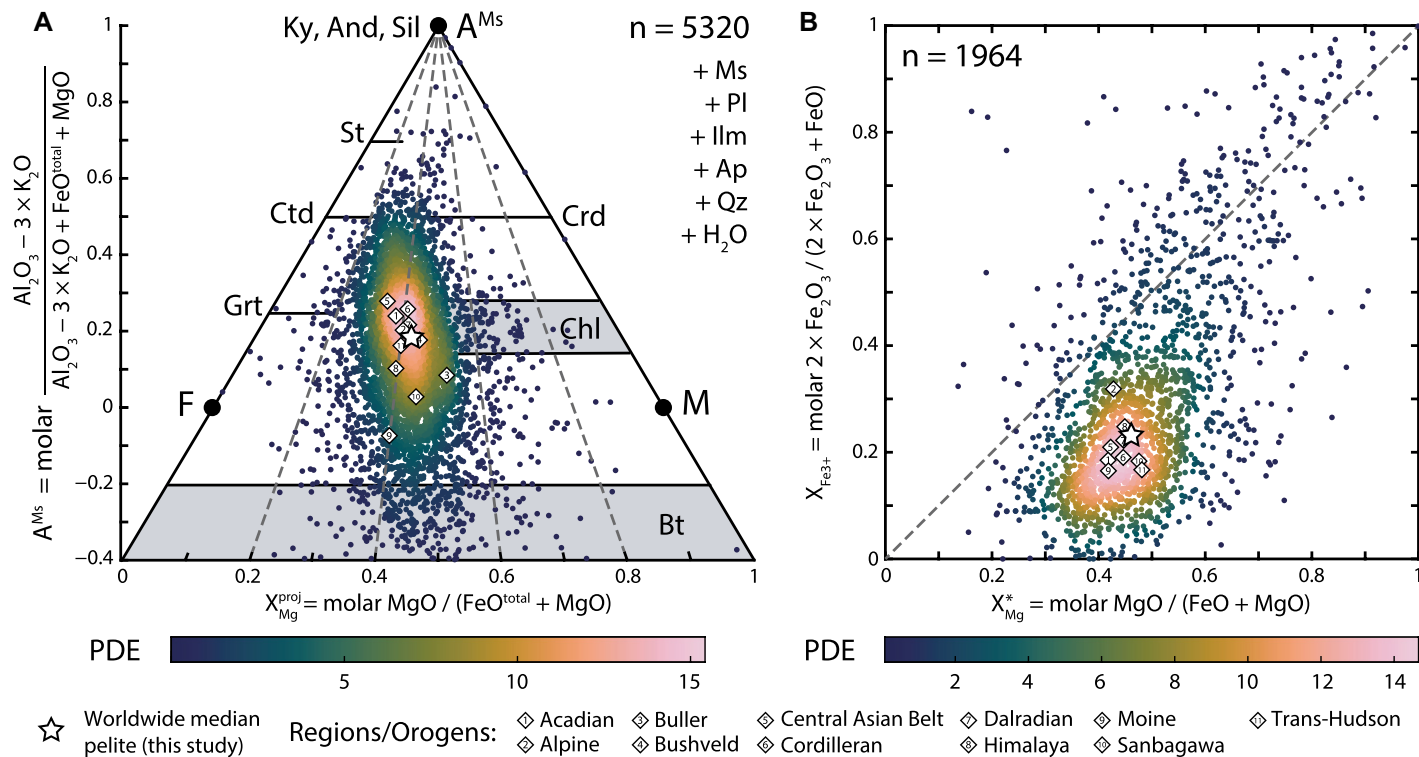
Figure 2. (A) 5320 analyses plotted on Al_2O_3-FeO-MgO (AFM) diagram after projection from muscovite and other phases (+). (B) Plot of X_{Fe3+} versus X_{Mg}^* for 1964 analyses for which FeO was measured using titration. Median worldwide pelite composition (star) and median composition from different regions and/or orogens are shown. Database analyses were colored using the "batlow" color scheme (Crameri, 2021) according to probability density estimates (PDE). Mineral abbreviations are after Warr (2021).

the highest density at $X_{Mg}^* \sim 0.4$ and $X_{Fe3+} \sim 0.2$. The median worldwide pelite has X_{Fe3+} of 0.23 and X_{Mg}^* of 0.46 based on these 1964 samples, compared to X_{Mg} of 0.39 [X_{Mg} = molar MgO/ $(MgO + FeO^{total})$] for all 5729 samples assuming all iron is FeO (Table 1).

Regional Analysis

In order to determine if it is justified to use the above median pelite composition to compare *P-T* conditions in different metamorphic belts, we calculated median compositions for 11 regions and/or orogens in the database for which there were more than 100 analyses. Most of these regional median values clustered together, with compositions similar to the worldwide median pelite (Fig. 2; Table 1). Exceptions included the Moine (Scotland) and Sanbagawa (Japan) regions, which had lower A^{Ms} values, the Buller (New Zealand) region, which had higher X_{Mg}, and the Alpine (Austria, Italy, and Switzerland) region, which had higher X_{Fe3+}.

Metamorphic Grade

Previous authors have reported a decrease in both volatile content and X_{Fe3+} with increasing metamorphic grade (Shaw, 1956; Ague, 1991). We found a consistent decrease in LOI across all nine zones, and a decrease in X_{Fe3+} from the diagenetic to biotite zone (Fig. 3). In order to assess grade-related variations in the other major elements, analyses were normalized to 100% on

a volatile-free basis with all iron converted to FeO. With a few exceptions, the major elements showed little consistent variation with metamorphic grade. Pelites from the porphyroblast and subsolidus sillimanite or K-feldspar zones showed lower median SiO_2 contents and higher median TiO_2 and Al_2O_3 contents compared to higher- and lower-grade zones. Median MnO contents of the garnet zone were elevated compared to other zones. Median K_2O contents were relatively constant across metamorphic grade. Samples from the diagenetic, anchizone, chlorite, porphyroblast, and subsolidus sillimanite or K-feldspar zones gave higher median A^{Ms} values than those of the biotite, garnet, migmatite, and garnet-cordierite zones (Fig. 3B).

DISCUSSION

While pelitic compositions occur over a range of AFM values, there is a strong clustering of analyses at $X_{Mg}^{proj} \sim 0.4$ and $A^{Ms} \sim 0.2$, with no separation between high- and low-Al pelites (Fig. 2A). AFM values for most regions cluster together (Fig. 2; Table 1), implying that it is justified to compare the inferred *P-T* conditions of commonly occurring metapelitic mineral assemblages between different orogens. An unexpected result of our study is the relatively high median whole-rock X_{Fe3+} of 0.23, given that X_{Fe3+} in oxides and silicates in metapelites other than hematite, magnetite, and muscovite are lower than this value, and muscovite has low

absolute Fe^{3+} (Forshaw and Pattison, 2021). This question requires further study.

Previous studies differ concerning whether there is significant bulk compositional change in major elements as a function of metamorphic grade: Some authors have argued for progressive change in bulk composition with increasing grade (Lapadu-Hargues, 1945; Ague, 1991, 1997), while others have argued that metamorphism is essentially isochemical apart from the loss of volatiles and reduction of iron (Shaw, 1956; Vidale, 1974; Atherton and Brotherton, 1982; Walther et al., 1995; Moss et al., 1996; Stepanov, 2021). While we found a continuous decrease in volatile content across the full range of metamorphic grades, median X_{Fe3+} only decreased markedly from the diagenetic to biotite zones and remained relatively constant at higher grades (Fig. 3). After accounting for these differences by normalizing analyses to 100% on a volatile-free basis with all iron converted to FeO, there were still distinct differences in concentrations of elements for certain metamorphic zones. Examples include lower median SiO_2 and higher median Al_2O_3 and A^{Ms} for the porphyroblast and subsolidus sillimanite or K-feldspar zones, and higher median MnO in the garnet zone.

Ague (2011, 2017) demonstrated that mass transfer is an important process in domains of high fluid flux and more minor away from these domains. While our database excluded samples
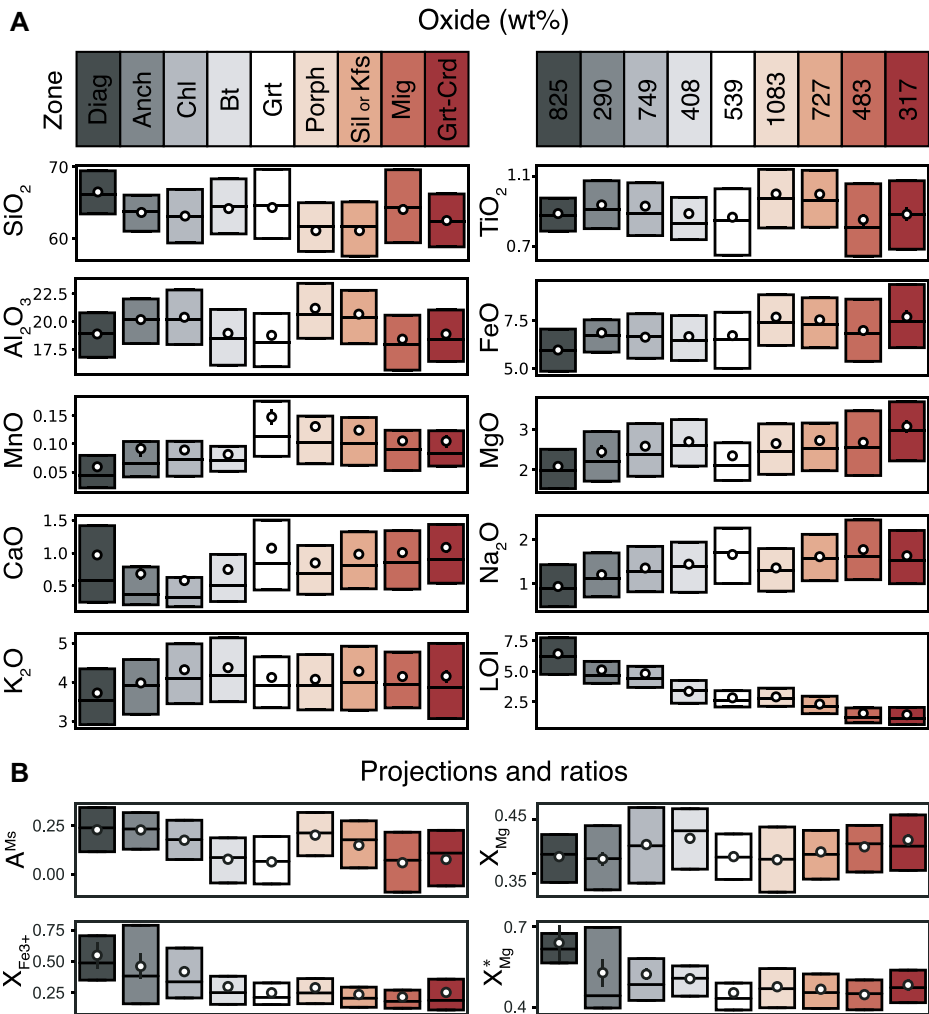
Figure 3. Changes in composition as function of metamorphic grade. (A) Elemental oxides and loss-on-ignition (LOI) in weight percent. (B) A^{Ms}, X_{Mg}, X_{Fe3+}, and X^*_{Mg}. For each category, box shows median and interquartile range, white circle represents the mean value, and error bar denotes the standard error (2σ). See Figure 1 for zone abbreviations.

lecting and sectioning pelitic rocks, minimum variance specimens were emphasized, so that samples were biased in favor of rocks containing several of the phases staurolite, garnet, sillimanite, andalusite, and cordierite" (Holdaway et al., 1982, p. 574).

Despite the above considerations, the size of our database and the fact that it incorporated a wide range of metamorphic grades and geographic locations mean that analyses were not skewed toward a single metamorphic zone. Therefore, phase diagram modeling using the median worldwide pelite presented in this paper (Table 1) should allow broad comparison of the *P-T* conditions of different pelitic mineral assemblages and of different metamorphic terrains.

REFERENCES CITED
Ague, J.J., 1991, Evidence for major mass transfer and volume strain during regional metamorphism of pelites: Geology, v. 19, p. 855–858, https://doi.org/10.1130/0091-7613(1991)019<0855:EFMMTA>2.3.CO;2.

Ague, J.J., 1997, Compositional variations in metamorphosed sediments of the Littleton Formation, New Hampshire—Discussion: American Journal of Science, v. 297, p. 440–449, https://doi.org/10.2475/ajs.297.4.440.

Ague, J.J., 2011, Extreme channelization of fluid and the problem of element mobility during Barrovian metamorphism: The American Mineralogist, v. 96, p. 333–352, https://doi.org/10.2138/am.2011.3582.

Ague, J.J., 2017, Element mobility during regional metamorphism in crustal and subduction zone environments with a focus on the rare earth elements (REE): The American Mineralogist, v. 102, p. 1796–1821, https://doi.org/10.2138/am-2017-6130.

described as or interpreted to have been affected by metasomatism, the low SiO_2 values in the porphyroblast and subsolidus sillimanite or K-feldspar zones could result in part from the increase in silica solubility with metamorphic grade (Manning, 1994). Alternatively, differences may be explained by sampling bias, in which especially aluminous layers containing abundant, petrologically significant porphyroblasts may have been preferentially sampled by petrologists in the field (e.g., Walther et al., 1995; Stepanov, 2021). The preferential sampling by metamorphic petrologists is perhaps best exemplified by the following quote: "In col-

TABLE 1. MEDIAN PELITE COMPOSITIONS

Region or Orogen	n	SiO_2	TiO_2	Al_2O_3	FeO	MnO	MgO	CaO	Na_2O	K_2O	X_{Mg}	X_{Fe3+}	X^*_{Mg}	A^{Ms}	X^{proj}_{Mg}
		(wt%)									(calculated from mol% values)				
Worldwide	5729 (1964)	64.13	0.91	19.63	6.85	0.08	2.41	0.65	1.38	3.95	0.39	0.23	0.46	0.19	0.42
Acadian	403 (56)	62.93	1.05	20.22	7.26	0.11	2.47	0.53	1.31	4.11	0.38	0.18	0.42	0.21	0.41
Alpine	134 (69)	61.41	1.00	21.41	7.72	0.11	2.32	0.79	1.28	3.97	0.35	0.32	0.43	0.24	0.38
Buller	137 (0)	65.29	0.76	18.44	6.15	0.05	3.37	0.37	1.16	4.41	0.50	N.A.	N.A.	0.09	0.52
Bushveld	132 (0)	63.56	0.79	19.14	7.71	0.06	3.22	0.62	1.05	3.85	0.43	N.A.	N.A.	0.18	0.45
Central Asian belt	119 (69)	63.06	0.99	20.49	7.68	0.11	2.06	0.83	1.26	3.52	0.32	0.21	0.42	0.28	0.35
Cordilleran	329 (127)	63.73	0.95	20.20	6.99	0.08	2.41	0.68	1.09	3.85	0.38	0.19	0.45	0.26	0.41
Dalradian	862 (605)	60.47	1.08	21.28	7.84	0.10	2.78	0.72	1.73	4.00	0.39	0.22	0.45	0.21	0.42
Himalayan	192 (86)	66.56	0.71	18.41	6.15	0.07	2.03	0.53	1.20	4.34	0.37	0.25	0.45	0.10	0.40
Moine	102 (24)	61.24	1.01	19.20	7.32	0.12	2.40	2.30	2.52	3.89	0.37	0.17	0.42	−0.07	0.40
Sanbagawa	148 (6)	70.60	0.60	15.87	4.61	0.15	1.89	0.67	2.24	3.38	0.42	0.18	0.48	0.03	0.45
Trans-Hudson	128 (25)	64.42	0.76	18.87	7.29	0.07	2.54	0.73	1.52	3.80	0.38	0.17	0.48	0.16	0.41

Note: All iron is shown as FeO^{total} with volatiles (loss-on-ignition [LOI], H_2O, CO_2, and SO_3) removed and values renormalized to 100%. X_{Mg}, X_{Fe3+}, X^*_{Mg}, A^{Ms}, and X^{proj}_{Mg} are defined in the text; *n*—number of analyses. Number in parentheses is the number of analyses with measured FeO and Fe_2O_3. See the Supplemental Material (see text footnote 1) for locations of each region.

Aitchison, J., 1982, The statistical analysis of compositional data: Journal of the Royal Statistical Society: Series B (Methodological), v. 44, p. 139–160, https://doi.org/10.1111/j.2517-6161.1982.tb01195.x.

Atherton, M.P., and Brotherton, M.S., 1982, Major element composition of the pelites of the Scottish Dalradian: Geological Journal, v. 17, p. 185–221, https://doi.org/10.1002/gj.3350170303.

Barrow, G., 1893, On an intrusion of muscovite-biotite gneiss in the south-eastern highlands of Scotland, and its accompanying metamorphism: Quarterly Journal of the Geological Society, London, v. 49, p. 330–358, https://doi.org/10.1144/GSL.JGS.1893.049.01-04.52.

Caddick, M.J., and Thompson, A.B., 2008, Quantifying the tectono-metamorphic evolution of pelitic rocks from a wide range of tectonic settings: Mineral compositions in equilibrium: Contributions to Mineralogy and Petrology, v. 156, p. 177–195, https://doi.org/10.1007/s00410-008-0280-6.

Chayes, F., 1960, On correlation between variables of constant sum: Journal of Geophysical Research, v. 65, p. 4185–4193, https://doi.org/10.1029/JZ065i012p04185.

Crameri, F., 2021, Scientific Colour Maps, Version 7.0.0: https://doi.org/10.5281/zenodo.4491293, (accessed January 2021).

Forshaw, J.B., and Pattison, D.R.M., 2021, Ferrous/ferric (Fe^{2+}/Fe^{3+}) partitioning among silicates in metapelites: Contributions to Mineralogy and Petrology, v. 176, 63, https://doi.org/10.1007/s00410-021-01814-4.

Hietanen, A., 1967, On the facies series in various types of metamorphism: The Journal of Geology, v. 75, p. 187–214, https://doi.org/10.1086/627246.

Holdaway, M.J., Guidotti, C.V., Novak, J.M., and Henry, W.E., 1982, Polymetamorphism in medium- to high-grade pelitic metamorphic rocks, west-central Maine: Geological Society of America Bulletin, v. 93, p. 572–584, https://doi.org/10.1130/0016-7606(1982)93<572:PIMTHP>2.0.CO;2.

Lapadu-Hargues, P., 1945, Sur l'existence et la nature de l'apport chimique dans certaines séries cristallophylliennes: Bulletin de la Société Géologique de France, v. S5-XV, p. 255–310, https://doi.org/10.2113/gssgfbull.S5-XV.4-6.255.

Mahar, E.M., Baker, J.M., Powell, R., Holland, T.J.B., and Howell, N., 1997, The effect of Mn on mineral stability in metapelites: Journal of Metamorphic Geology, v. 15, p. 223–238, https://doi.org/10.1111/j.1525-1314.1997.00011.x.

Manning, C.E., 1994, The solubility of quartz in H_2O in the lower crust and upper mantle: Geochimica et Cosmochimica Acta, v. 58, p. 4831–4839, https://doi.org/10.1016/0016-7037(94)90214-3.

Merriman, R.J., and Frey, M., 1999, Patterns of very low-grade metamorphism in metapelitic rocks, in Frey, M., and Robinson, D., eds., Low-Grade Metamorphism: Oxford, UK, Blackwell Science, p. 61–107, https://doi.org/10.1002/9781444313345.ch3.

Moss, B.E., Haskin, L.A., and Dymek, R.F., 1996, Compositional variations in metamorphosed sediments of the Littleton Formation, New Hampshire, and the Carrabassett Formation, Maine, at sub-hand specimen, outcrop, and regional scales: American Journal of Science, v. 296, p. 473–505, https://doi.org/10.2475/ajs.296.5.473.

Pattison, D.R.M., and Spear, F.S., 2018, Kinetic control of staurolite-Al_2SiO_5 mineral assemblages: Implications for Barrovian and Buchan metamorphism: Journal of Metamorphic Geology, v. 36, p. 667–690, https://doi.org/10.1111/jmg.12302.

Pattison, D.R.M., and Tracy, R.J., 1991, Phase equilibria and thermobarometry of metapelites, in Kerrick, D.M., ed., Contact Metamorphism: Berlin, De Gruyter, p. 105–206, https://doi.org/10.1515/9781501509612-007.

Rock, N.M.S., 1988, Summary statistics in geochemistry: A study of performance of robust estimates: Mathematical Geology, v. 20, p. 243–275, https://doi.org/10.1007/BF00890256.

Rollinson, H.R., and Pease, V., 2021, Using Geochemical Data: To Understand Geological Processes: Cambridge, UK, Cambridge University Press, 346 p., https://doi.org/10.1017/9781108777834.

Shaw, D., 1956, Geochemistry of pelitic rocks: Part III. Major elements and general geochemistry: Geological Society of America Bulletin, v. 67, p. 919–934, https://doi.org/10.1130/0016-7606(1956)67[919:GOPRPI]2.0.CO;2.

Spear, F.S., 1993, Metamorphic Phase Equilibria and Pressure-Temperature-Time Paths: Washington, D.C., Mineralogical Society of America, 799 p.

Stepanov, A.S., 2021, A review of the geochemical changes occurring during metamorphic devolatilization of metasedimentary rocks: Chemical Geology, v. 568, https://doi.org/10.1016/j.chemgeo.2021.120080.

Thompson, J.B., 1957, The graphical analysis of mineral assemblages in pelitic schists: American Journal of Science, v. 42, p. 842–858.

Tinkham, D.K., Zuluaga, C.A., and Stowell, H.H., 2001, Metapelite phase equilibria modeling in MnNCKFMASH: The effect of variable Al_2O_3 and MgO/(MgO + FeO) on mineral stability: Geological Materials Research, v. 3, p. 1–42.

Vidale, R., 1974, Metamorphic differentiation layering in pelitic rocks of Dutchess County, New York, in Hojmann, A.W., et al., eds., Geochemical Transport and Kinetics: Washington, D.C., Carnegie Institution of Washington, p. 273–286.

Walther, J.V., Holdaway, M.J., and Ague, J.J., 1995, Mass transfer during Barrovian metamorphism; Discussion and reply: American Journal of Science, v. 295, p. 1020–1033, https://doi.org/10.2475/ajs.295.8.1020.

Warr, L.N., 2021, IMA-CNMNC approved mineral symbols: Mineralogical Magazine, v. 85, p. 291–320, https://doi.org/10.1180/mgm.2021.43.

White, R.W., Powell, R., Holland, T.J.B., Johnson, T.E., and Green, E.C.R., 2014, New mineral activity-composition relations for thermodynamic calculations in metapelitic systems: Journal of Metamorphic Geology, v. 32, p. 261–286, https://doi.org/10.1111/jmg.12071.

Woronow, A., and Love, K.M., 1990, Quantifying and testing differences among means of compositional data suites: Mathematical Geology, v. 22, p. 837–852, https://doi.org/10.1007/BF00890666.